



# Active laser medium for near-infrared spectral range based on electron-unsymmetrical polymethine dye and silver nanoparticles

Niazbek Ibrayev<sup>1</sup> · Alexander Ishchenko<sup>2</sup> · Dmitriy Afanasyev<sup>1,3</sup> · Nazerke Zhumabay<sup>1</sup>

Received: 17 April 2019 / Accepted: 23 August 2019 / Published online: 31 August 2019  
© Springer-Verlag GmbH Germany, part of Springer Nature 2019

## Abstract

An effect of silver nanoparticles (Ag NPs) on spectral luminescent and lasing properties of an electron-unsymmetrical polymethine dye in ethanol solution has been studied. Fluorescence of the dye is characterized by a large Stokes shift of  $3007\text{ cm}^{-1}$  and a quantum yield  $\Phi_f$  of 0.08. An increase in the absorption cross section and in the fluorescence quantum yield of the dye molecules is observed in the presence of Ag NPs. The dye fluorescence lifetime of 1.11 ns remains unchanged after the addition of Ag NPs to the solution. Stimulated emission with spectrally pronounced two-mode oscillations has been obtained for the dye in the region of its fluorescence band maximum. A stimulated emission threshold is achieved on the average at  $3.35\text{ MW/cm}^2$ . The presence of Ag NPs leads to the enhanced intensity and 28% lowered threshold of dye stimulated emission. The data obtained can be used to develop new near-infrared lasing media.

## 1 Introduction

Polymethine dyes are unique light energy converters, because they have the greatest range of changes in photo-physical and nonlinear optical properties among organic chromophores [1–6]. Therefore, they are widely used both as active media [2, 7] and as passive Q-switches [2, 8]. Electron-unsymmetrical polymethine dyes are most promising for lasing, since they have significantly broader absorption bands and larger fluorescence Stokes shifts compared with the corresponding symmetric dyes [9, 10]. The former feature of unsymmetrical dyes allows the use of one dye instead of a set of dyes for different pump sources, whereas the latter feature enables ultraviolet and visible light to be converted to practically important infrared (IR) radiation using common lasers of the visible range, for example, the second-harmonic generation of a neodymium laser [2]. The stronger electron

asymmetry of a dye, the broader is the absorption band and the larger is the Stokes shift [9]. However, it is preferable for a dye to have an optimum (medium) electron asymmetry; if it is too strong, vibronic interactions in molecules are enhanced to a degree sufficient to significantly quench fluorescence [2, 9]. This effect can become crucial in the near-IR range where the fluorescence efficiency of organic dyes is dramatically reduced due to enhanced internal conversion (according to the energy gap law [1]). At wavelengths above 750 nm, internal conversion is so efficient that it cancels even a significant potential increase in fluorescence quantum yield which could be achieved by dye structure optimization [1]. Therefore, it is challenging to explore other than structure-optimizing approaches for stronger luminescence of polymethine dyes. They can be exemplified by a method invoking the plasmonic effects induced by nanoparticles (NPs) of noble metals [11].

Plasmonic properties of metal nanostructures are known to change radically with their size and shape. To numerically investigate the plasmonic effect in nanostructures, the finite difference method has been applied [12–17]. For instance, it enabled elucidation of plasmonic effect characteristics in core-shell nanostructures [12–14], nanopearls [15], nanobowties [16], and more complex nanostructure arrays [17]. Other methods were also used in such studies [18, 19]. However, the preparation of the nanostructures concerned represents a rather complex process.

✉ Dmitriy Afanasyev  
a\_d\_afanasyev@mail.ru

<sup>1</sup> Institute of Molecular Nanophotonics, Buketov Karaganda State University, Universitetskaya 28, 100028 Karaganda, Kazakhstan

<sup>2</sup> Institute of Organic Chemistry, National Academy of Sciences of Ukraine, Murmanskaya, 5, Kiev 02094, Ukraine

<sup>3</sup> Institute of Applied Mathematics, Universitetskaya 28A, 100028 Karaganda, Kazakhstan

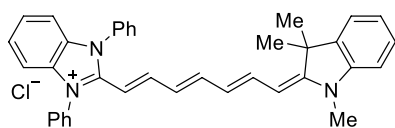
The presence of plasmonic metal NPs can result in the increased absorption cross section and more intense fluorescence of organic molecules. These effects can be harnessed to create optoelectronic devices [20], nanolasers [21], sensors [22], etc.

The influence of metal NPs on the stimulated light emission of some laser dyes was studied previously [21, 23–26]. The plasmonic effect was found to lower the stimulated emission threshold. It was also shown that, along with the plasmonic effect, the scattering of exciting radiation by metal NPs contributes to a decrease in the lasing threshold [25, 27].

The present work is aimed to study the spectral luminescent and lasing properties of electron-unsymmetrical polymethine dye **1** in the presence of silver nanoparticles.

## 2 Experimental

Polymethine **1** was chosen as an electron-unsymmetrical dye.



Dye **1** was prepared according to the method described in [28], by boiling a mixture of equimolar amounts of 2-methyl-1,3-diphenylbenzimidazolium chloride and 1,3,3-trimethyl-2-(6-acetylanilino-1,3,5-hexatrienyl)-3H-indolium perchlorate in pyridine in the presence of a triethylamine condensing

agent. The dye was precipitated from the reaction mixture with an aqueous solution of sodium perchlorate. The product was purified by chromatography on aluminium oxide from chloroform. The impurities were eluted with benzene, and the dye was then eluted with chloroform. After evaporation of the solvent, the dye was reprecipitated from acetonitrile with an aqueous solution of sodium tetrafluoroborate. Dye **1** has a medium electron asymmetry, thus promising sufficient luminescence efficiency. In addition, the probability of absorption from the  $S_1$  state to higher excited states is insignificant, and hence should not reduce the generation efficiency [29]. Dye **1** is highly soluble in ethanol and has high photochemical resistance.

Ag NPs in ethanol were obtained by ablation of the silver target by the second harmonic of a solid-state Nd:YAG laser ( $\lambda_{\text{gen}} = 532$  nm,  $\tau = 10$  ns,  $E = 90$  mJ). The repetition rate of the pulse packet was 20 Hz and the ablation time was 10 min. Each laser pulse packet was focused on different parts of the target surface. The volume of ethanol in the target cell was  $V = 2$  ml and the thickness of the ethanol layer above the surface was 6 mm. The size of Ag NPs in colloidal solutions was determined by dynamic light scattering on the submicron particle size analyzer Zetasizer Nano ZS (Malvern). The average size of the Ag NPs was 32 nm and the standard deviation was 10 nm (Fig. 1). Ag NPs concentration in solution was determined using the formula:

$$\Delta N = \Delta m / m, \quad (1)$$

where  $\Delta m$  is the difference in mass of the target before and after ablation and  $m$  is the average mass of one particle ( $m = \rho V$ , where  $V$  is the average volume of NP and  $\rho$  is the target material density). Based on the obtained value and

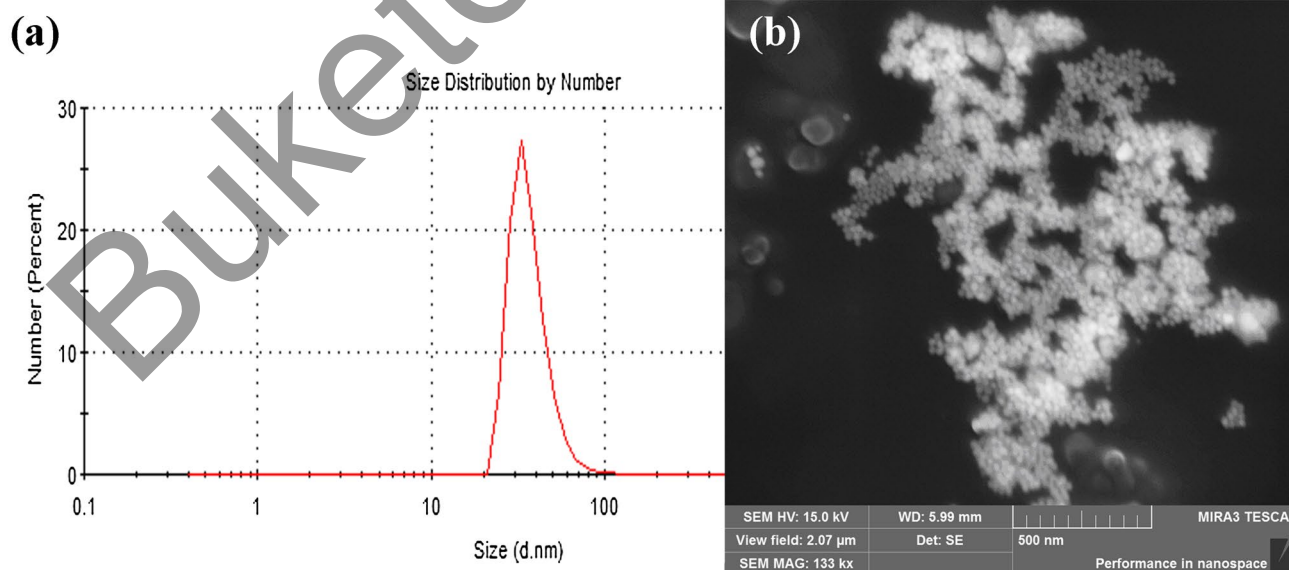


Fig. 1 Ag NPs size distribution (a) and their electron microscopic image (b)

volume of solutions, the number of NPs per unit volume was calculated. The concentration of Ag NPs in the working solution was  $C_{Ag} = 10^{-10}$  mol/L. The average distance between the NPs was determined on the assumption that the nanoparticles are equidistant from each other and the spheres in the centers of which they are located form the most dense package. To obtain the volume of individual spheres, we multiplied the volume per single NPs by the coefficient 0.74048. Then the radius of the sphere was calculated by the formula  $r = \sqrt[3]{3V/4\pi}$ . The average distance between the nanoparticles ( $D_{NPs}$ ) in the solution was obtained by multiplying the value obtained by 2.

The dye concentration in the solution was constant and equal to  $10^{-4}$  mol/L.

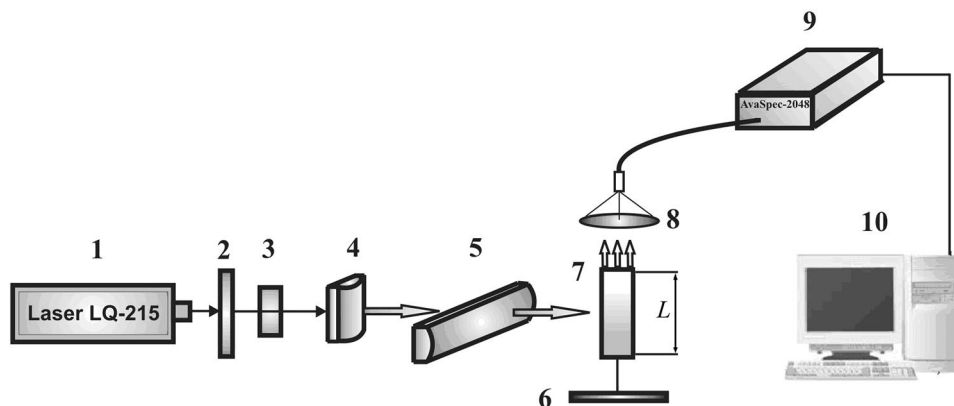
Absorption spectra were recorded on a Cary 300 spectrophotometer (Agilent) and fluorescence spectra were recorded on an Eclipse spectrofluorometer (Agilent).

The quantum yield of fluorescence  $\Phi_f$  was measured by the absolute method. AvaSphere 30-REFL integrating sphere and AvaSpec-ULS2048 spectrometer were used for measurement. LCS-DTL-374QT laser ( $\lambda_{gen} = 532$  nm,  $\tau = 7$  ns,  $E = 20$   $\mu$ J) was used as a monochromatic light source. To measure the absolute quantum yield of fluorescence, a reference cell with a solvent and a cell with a dye solution were alternately placed inside the integrating sphere in the irradiating flow of monochromatic radiation. The absolute quantum yield was estimated according to the formula [30]:

$$\Phi_f = \frac{PN(Em) \int \frac{\lambda}{hc} [I_{em}^{sample}(\lambda) - I_{em}^{reference}(\lambda)] d\lambda}{PN(Abs) \int \frac{\lambda}{hc} [I_{ex}^{reference}(\lambda) - I_{ex}^{sample}(\lambda)] d\lambda}, \quad (2)$$

where PN(Abs) is the number of photons absorbed by the sample, PN(Em) the number of photons emitted by the sample,  $\lambda$  the wavelength,  $h$  the Planck constant,  $c$  the light velocity,  $I_{ex}^{reference}$  and  $I_{ex}^{sample}$  are the integral excitation light intensities with and without the dye molecules in the cell with the solvent, respectively.

**Fig. 2** Schematic diagram of apparatus for the study of generation characteristics: (1) LQ 215 laser, (2) neutral filters, (3) diaphragm, (4, 5) cylindrical lenses, (6) blind mirror, (7) test sample, (8) collecting lens, (9) AvaSpec-2048 spectrometer, (10) computer



When measuring the characteristics of laser generation, an optical resonator is used, which is formed by a blind mirror (6) and the front face of the cell with a dye solution (7) (Fig. 2). The distance from the center of the cuvette to the mirror was 70 mm. The radiation of the pump passing the diaphragm (3) with the help of cylindrical lenses (4, 5) was focused on the side face of the cuvette in a strip of  $0.07$   $cm^2$ . Lasing arises in a narrow region near the entrance wall of the cuvette. Quartz cuvettes made of the KU-1 brand composition were used in the work. The cuvettes with dye solutions were fixed on a steel holder.

The pump power density varied with the help of neutral filters (2) and was  $2-9$   $MW/cm^2$ . The radiation from the collecting lens (8) was focused on the optical fiber input of the AvaSpec-2048 spectrometer (9). The relative error of spectral characteristics determination was 3%.

To study the effect of the optical path length of the cuvette ( $L$ , Fig. 2) on the stimulated emission spectrum of dye 1, a series of cuvettes with  $L$  equal to 1, 3, 5, 10, 20 mm were used.

### 3 Results and discussion

Figure 3 shows the absorption spectra of Ag NPs (curve 1), dye 1 (curve 2), and fluorescence of dye 1 (curve 3). The absorption spectrum of dye 1 appears as a broad band with a maximum at 610 nm and a full width at half maximum ( $FWHM$ ) of  $166$   $cm^{-1}$ . The fluorescence band with a maximum at 750 nm and  $FWHM$  of  $60$   $cm^{-1}$  has a significant Stokes shift of  $3007$   $cm^{-1}$ .

The absorption spectrum of Ag NPs in ethanol with a maximum at 400 nm overlaps with the absorption spectrum of dye 1, thus indicating that the resonance conditions between the absorption spectra of Ag NPs and the dye are satisfied.

Dye 1 absorption and fluorescence band positions and  $FWHMs$  remain unchanged after the addition of all

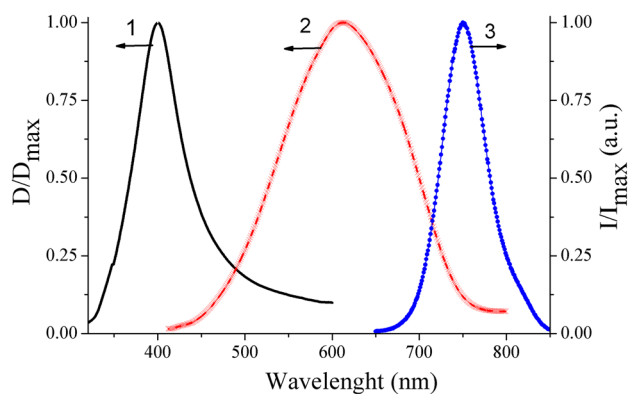


**Fig. 3** Absorption spectra of Ag NPs (1) and dye **1** (2), and the fluorescence spectrum of dye **1** (3) in ethanol

concentrations of Ag NPs. This rules out both dye molecules aggregation and formation of nanoparticle–dye complexes in solutions.

The effects of Ag NPs concentration on the optical density  $D$  (curve 1) and fluorescence intensity (curve 2) of dye **1** are shown in Fig. 4.

The optical density  $D$  of the dye depends non-monotonically on the concentration of Ag NPs in the solution (Fig. 4). The dye absorption is enhanced at low Ag NPs concentrations. The value  $D$  increased by 1.2 times at the NPs concentration equal to  $10^{-12}$  mol/L. As the Ag NPs concentration grows further, the optical density is slightly reduced. The ascending branch of curve 1 corresponding to the growing dye absorption is attributed to an increase in the absorption cross section caused by the local optical field strength near the surface of metal NPs. The enhancement effect in the dye absorption grows with the increasing number of Ag NPs around the dye molecules until saturation occurs. However, an increased concentration of plasmonic NPs can also result

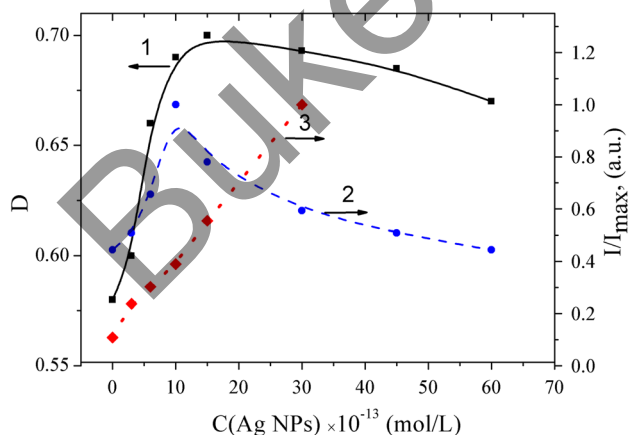
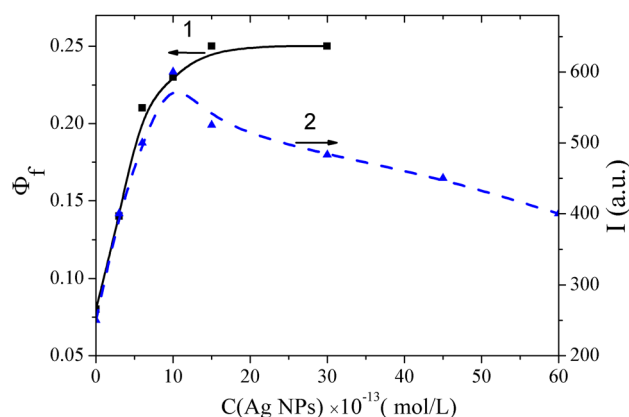


**Fig. 4** The effect of Ag NPs concentration on the optical density (1) and fluorescence intensity (2) of dye **1**, and on the scattering intensity (3) of laser beam ( $\lambda = 532$  nm)

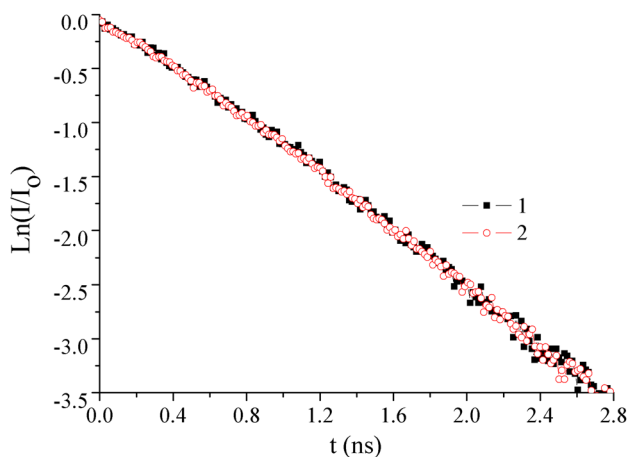
in a weakened field strength, thus leading to a decrease in the dye absorption coefficient [31]. Dye fluorescence enhances until the Ag NPs concentration  $C_{Ag}$  is up to  $10^{-12}$  mol/L, with the maximum intensity 2.2 times as large as that without NPs. A further increase in  $C_{Ag}$  leads to luminescence quenching. The increase in the fluorescence intensity of the dye from the local field of Ag NPs is associated with both an increment in the number of singlet excited  $S_1$  molecules and a growth of the fluorescence quantum yield ( $\Phi_f$ ) when the plasmon resonance was applied to the dye molecules.

Figure 5 shows the dependence of  $\Phi_f$  (curve 1) of the dye on the concentration of Ag NPs. The fluorescence quantum yield was equal to  $\Phi_f = 0.08$  for the dye in the ethanol without NPs. The increase in  $\Phi_f$  in the presence of Ag NPs indicates an increase in the rate of the radiative transition of the dye molecules from  $S_1$  state to  $S_0$ . Reaching the maximum value of the  $\Phi_f$  curve after  $C_{Ag} = 10^{-12}$  mol/L suggests that under these conditions the action of the local field of Ag NPs reaches a maximum value. The fluorescence was quenched at the concentration of Ag NPs more than  $C_{Ag} = 10^{-12}$  mol/L. It can result in both weakening of the local field strength of Ag NPs and energy transfer from excited dye molecules to metal nanoparticles [11], when metal nanoparticles and dye molecules approach to each other up to contact.

Decay kinetics of the dye fluorescence intensity were measured by the time-correlated single photon counting method on the Simple-Tau 150 system (Becker & Hickl GmbH). Fluorescence of the samples was excited by using a pulsed semiconductor laser with a lasing wavelength of  $\lambda_{gen} = 488$  nm with a pulse duration at half-height  $\tau = 150$  ps. Analysis of the fluorescence decay curves using the SPCImage software showed that the attenuation of the luminescence of the dye occurs exponentially with  $\tau_{fl} = 1.11$  ns [32]. Upon the addition of Ag NPs to the solution, the duration of fluorescence is almost unchanged (Fig. 6).



**Fig. 5** Effect of Ag NPs concentration on fluorescence quantum yield  $\Phi_f$  (1) and stimulated emission intensity (2) of dye **1**



**Fig. 6** Fluorescence decay kinetics of dye **1** with and without Ag NPs. 1:  $C_{Ag}=0$  mol/L; 2:  $C_{Ag}=10^{-12}$  mol/L

An increase in the fluorescence rate constant should have led to a decrease in the lifetime of the excited state  $S_1$ . However, measurements have shown that at different concentrations of Ag NPs, the  $\tau_{fl}$  dye does not change. This is possible if, in the presence of metal NPs, along with an increase in the efficiency of the radiative decay channel, the non-radiative deactivation of the  $S_1$  state is attenuated [31].

For pulsed coherent-pumped dye lasers, the condition of single-frequency lasing can be written as inequality [33]:

$$\delta\lambda_{RES} \ll \lambda_0^2 / (2L_p), \quad (3)$$

where  $\delta\lambda_{RES}$  is the bandwidth of the resonator at the level of  $e^{-1}$  power,  $\lambda_0$  the wavelength corresponding to the maximum transmission of the resonator, and  $L_p$  is the optical length of the resonator. Numerical calculation by the formula (3) shows that the condition of single-frequency generation is not observed in our case.

The total number of resonant frequencies in the laser generation spectrum can be estimated using the formula [34]:

$$\Delta\omega = \pi c / L_p n, \quad (4)$$

where  $\Delta\omega$  is the difference between neighboring resonant frequencies,  $c$  the speed of light in the vacuum, and  $n$  is the refractive index of the medium, in the case of ethanol  $n=1.36$  [35]. By dividing line width gain on the value of  $\Delta\omega$ , it is possible to estimate the number of resonant frequencies in the generation spectrum. It is more than  $10^{10}$ . Therefore, multi-frequency generation of stimulated radiation of dye **1** in ethanol solution is possible.

Figure 7 presents the results of a study of the stimulated emission properties of dye **1** in ethanol. The length of the active medium in the quartz cuvette was 10 mm. Only spontaneous fluorescence of the dye with FWHM=42 nm (curve 1) is observed at a pump power density below 3 MW/cm<sup>2</sup>. When the power of the pump source reaches a value of

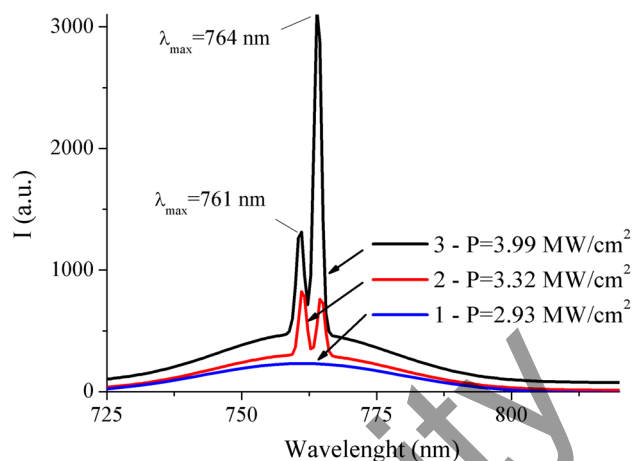


**Fig. 7** Emission spectra of the dye in ethanol at different pump power densities: 1:  $P=2.93$  MW/cm<sup>2</sup>, FWHM=42 nm; 2:  $P=3.32$  MW/cm<sup>2</sup>, FWHM=3 nm; 3:  $P=3.99$  MW/cm<sup>2</sup>, FWHM=2.5 nm

3.32 MW/cm<sup>2</sup>, a narrow band of laser radiation generation with FWHM=3 nm appears against the background of the fluorescence spectrum. The lasing spectrum has two maxima at wavelengths  $\lambda_1=761$  nm and  $\lambda_2=764$  nm (curve 2). A further increase in the power density of the pump source leads to an increase in the intensity of the lasing band and a decrease in its half-width (Fig. 7, curve 3). The narrowing of the radiation band with an increase in the excitation intensity indicates the predominance of stimulated radiation over spontaneous emission, i.e., the transition of the system to the generation mode.

The effect of the optical path length of the cuvette ( $L$ ) on the dye stimulated radiation spectrum was studied (Fig. 8). With a small length  $L$  ranging from 1 to 3 mm, only one

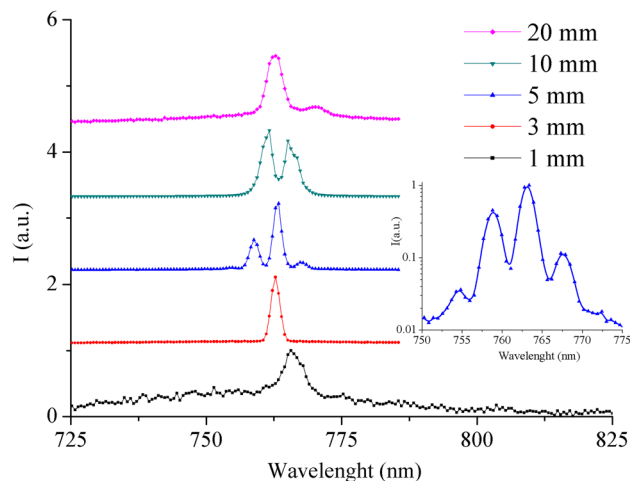


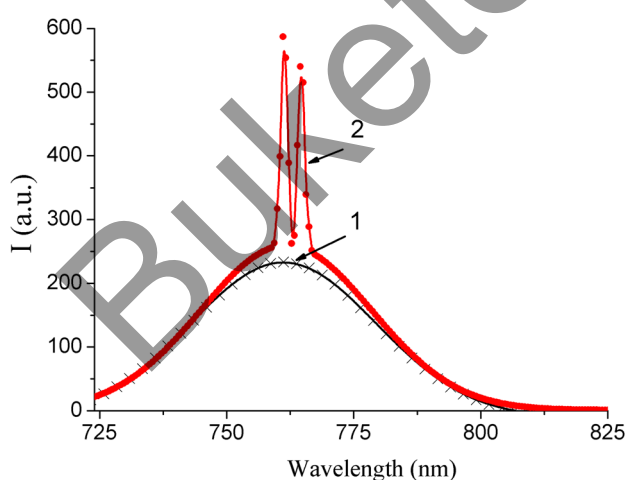
**Fig. 8** Lasing spectra of the dye **1** ( $C=10^{-4}$  mol/l) in ethanol at different length of cuvette  $L$ . Inset shows enlarged fragment of spectrum with  $L=5$  mm

**Table 1** The effect of optical path length on the peak position of stimulated radiation of polymethine dye 1 in ethanol

Optical path length in cuvettes, $L$ (mm)	$\lambda_1$ , nm	$\lambda_2$ , nm	$\lambda_3$ , nm	$\lambda_4$ , nm
1	–	–	766	–
3	–	–	763	–
5	755	759	763	768
10	–	761	764	–
20	–	–	763	770

peak at 766 and 763 nm is observed in the generation spectrum (Table 1), respectively. With the growth in the value of  $L$  to 5 mm in the spectrum of stimulated radiation of the dye, four peaks with intermode interval of  $\Delta\lambda \sim 4$  nm is observed. Further growth of  $L$  leads to the formation of two radiation peaks of luminescence (Fig. 8). It follows that the observed maxima in the generation spectrum are the modes of laser radiation.

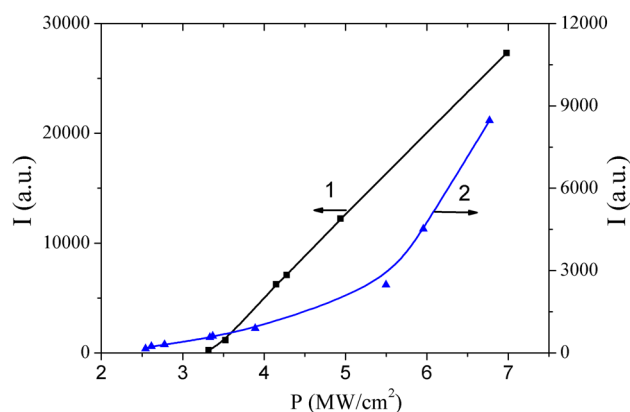
The effect of Ag NPs on the spectrum of stimulated radiation of the dye is shown in Fig. 9. Only the spontaneous fluorescence band was observed in the dye solution at the pump power densities of  $P = 2.93$  MW/cm<sup>2</sup> (curve 1). When a dye solution with Ag NPs is excited at the same pump power density, a laser generation band appears on the background of the fluorescence spectrum (curve 2). The addition of Ag NPs to the solution does not result in a change in the position of the dye's stimulated radiation peaks. This indicates that the formation of the mode composition of the stimulated radiation is mainly influenced by the length  $L$  of the optical path of the cuvettes.

**Fig. 9** Effect of Ag NPs on the stimulated radiation spectrum of dye 1 in ethanol: (1) emission spectra of the dye without Ag NPs; (2) emission spectra of the dye with Ag NPs. The pump power density is  $P = 2.93$  MW/cm<sup>2</sup>

The dependence of stimulated radiation intensity on the Ag NPs concentration is shown in Fig. 5 (curve 2). The obtained dependence almost completely repeats the dependence of the fluorescence intensity on the NPs concentration (Fig. 4, curve 2).

The dependence of the stimulated radiation intensity on the pump power density for the dye solution with Ag NPs concentration of  $C_{Ag} = 10^{-12}$  mol/L was studied in comparison with the solution without Ag NPs (Fig. 10). A linear dependence of the intensity of stimulated radiation on the pump power density was observed (curve 1) in the absence of Ag NPs. When adding in the active medium of plasmonic nanoparticles, the dependence of the intensity of stimulated emission has a complex form. In the range from 2.5 to 5.5 MW/cm<sup>2</sup>, there is a gradual increase in the radiation intensity, and then a more intensity growth dependence was registered. The threshold values of the dye pumping power in ethanol were determined from the obtained data. The lasing threshold value for the dye solution was 3.35 MW/cm<sup>2</sup>, and for the Ag NPs solution was 2.4 MW/cm<sup>2</sup>.

When the power density of pumping was more than 3.5 MW/cm<sup>2</sup>, intensity of stimulated radiation of the dye in solution without Ag NPs was higher in comparison with the generation of the solution containing Ag NPs. To explain the possible causes, the average distance between Ag NPs ( $D_{NPs}$ ) in the cell volume at the maximum particle concentration ( $C_{Ag}$ ) used in the work was estimated. With equal distribution, the average distance between Ag NPs was 20  $\mu$ m. This distance allows excluding from consideration the short-acting (non-plasmonic) effects connected with quenching of dye luminescence in the presence of Ag NPs. Therefore, one of the most likely reasons for this ratio between the intensities of stimulated radiation in solutions is due to the effects of scattering of exciting and stimulated radiation on Ag NPs. The increase in the scattering of the excitation light

**Fig. 10** Dependence of the intensity of dye 1 generation in ethanol without Ag NPs (1) and with Ag NPs  $C = 10^{-12}$  mol/L (2) on the pump power density

can have a positive effect on the generation process. When light is scattered, the length of the laser excitation path in the cuvette increases, which can increase the probability of light absorption by the dye and reduce the generation threshold. At the same time, the scattering of stimulated dye radiation in a solution with Ag NPs may lead to a decrease in the intensity of generation.

Almost the same dependence of the fluorescence intensity (Fig. 4, curve 2) and the intensity of the stimulated radiation (Fig. 5, curve 2) from the concentration of metal NPs indicates that the mechanisms of influence of localized plasmon resonance on stimulated and spontaneous radiation are identical.

The decrease in the stimulated emission threshold of the dye in the presence of Ag NPs is apparently due to both an increase in the fluorescence quantum yield and an increase in the scattering of exciting light in the active medium [24, 25].

## 4 Conclusions

Electron-unsymmetrical dye **1** in ethanol exhibits fluorescence with a large Stokes shift of  $3007\text{ cm}^{-1}$  and a quantum yield  $\Phi_f$  of 0.08. The localized plasmon resonance of Ag NPs leads to an increase in both the absorption cross section and the fluorescence quantum yield of the dye. The dye fluorescence lifetime of 1.11 ns remains unchanged after the addition of Ag NPs to the solution, thus suggesting that the localized plasmon resonance not only enhances the radiative decay channel but also weakens the non-radiative de-excitation.

Stimulated emission with spectrally pronounced two-mode oscillations has been obtained for dye **1** in the region of its fluorescence band maximum. A stimulated emission threshold is achieved on the average at  $3.35\text{ MW/cm}^2$ . Ag NPs give rise to the enhanced intensity and lowered threshold of dye stimulated emission. The results of the study show promise for the development of new near-infrared lasing media.

**Acknowledgements** This work was supported by the Committee of Science of the Ministry of Education and Science of the Republic Kazakhstan (Grant No. BR05236691).

## References

1. A.A. Ishchenko, Russian. Chem. Rev. **608**, 865 (1991)
2. A.A. Ishchenko, Q. Electron. **24**(6), 471 (1994)
3. R.A. Ganeev, R.I. Tugushev, A.A. Ishchenko, N.A. Derevyanko, A.I. Rysnyansky, T. Usmanov, Appl. Phys. B **76**, 683 (2003)
4. V.A. Svetlichnyi, A.A. Ishchenko, E.A. Vaitulevich, N.A. Derevyanko, A.V. Kulinich, Opt. Commun. **281**, 6072 (2008)
5. V. Voiciuk, K. Redeckas, N.A. Derevyanko, A.V. Kulinich, M. Barkauskas, M. Vengris, V. Sirutkaitis, A.A. Ishchenko, Dyes Pigments **109**, 120 (2014)
6. N.K. Ibrayev, E.V. Seliverstova, A.A. Ishchenko, M.A. Kudina, J. Photochem. Photobiol. A Chem. **346**, 570 (2017)
7. V.I. Bezrodnyi, A.A. Ishchenko, Appl. Phys. B **73**, 283 (2001)
8. V.I. Bezrodnyi, A.A. Ishchenko, Opt. Laser Technol. **34**, 7 (2002)
9. N.A. Derevyanko, A.A. Ishchenko, Yu.L. Slominski, A.I. Tolmachev, Mendeleev Commun. **3**, 91 (1991)
10. A.S. Tatikolov, N.A. Derevyanko, A.A. Ishchenko, I. Baraldi, M. Caselli, F. Momicchioli, G. Ponterini, Ber. Bunsenges. Phys. Chem. **99**, 763 (1995)
11. C.D. Geddes, J.R. Lakowicz, J. Fluor. **12**, 121 (2002)
12. Y.F. Chau, Y.J. Lin, D.P. Tsai, Opt. Express **18**, 3510–3518 (2010)
13. Y.F. Chou Chau, C.T. Chou Chao, H.J. Huang, Y.C. Wang, H.P. Chiang, M.N.S.M. Idris, Z. Masri, C.M. Lim, Res. Phys. **13**, 102290 (2019)
14. Y.F. Chau, Plasmonics **4**, 253 (2009)
15. Y.F. Chau, C.Y. Jheng, S.F. Joe, S.F. Wang, W. Yang, S.C. Jheng, Y.S. Sun, Y. Chu, J.H. Wei, J. Nanopart. Res. **15**, 1424 (2013)
16. W. Yang, Y.F. Chou Chau, S.C. Jheng, Phys. Plasmas **20**, 064503 (2013)
17. Y.F. Chou Chau, C.K. Wang, L.F. Shen, C.M. Lim, H.P. Chiang, C.T. Chou Chao, H.J. Huang, C.T. Lin, N.T.R.N. Kumara, N.Y. Voo, Sci. Rep. **7**, 16817 (2017)
18. B. Yun, Z. Wang, G. Hu, Y. Cui, Opt. Commun. **283**, 2947 (2010)
19. M. Arnold, M. Blaber, M. Ford, Opt. Express **22**(3), 3186 (2014)
20. M.A. Schmidt, A. Argyros, F. Sorin, Adv. Opt. Mater. **4**, 13 (2015)
21. V.I. Balykin, Phys. Usp. **61**, 846 (2018)
22. C.H. Lai, G.A. Wang, T.K. Ling, T.J. Wang, P.K. Chiu, Y.F. Chou Chau, C.C. Huang, H.P. Chiang, Sci. Rep. **7**, 5446 (2017)
23. NKh Ibrayev, A.K. Zeinidenov, Laser Phys. Lett. **11**, 115805 (2014)
24. NKh Ibrayev, A.K. Aimukhanov, Opt. Laser Technol. **115**, 246 (2019)
25. S. Ning, Z. Wu, N. Zhang, L. Ding, X. Hou, F. Zhang, Org. Electron. **50**, 403 (2017)
26. Y. Yin, T. Qiu, J. Li, P.K. Chu, Nano Energy **1**, 25 (2012)
27. W.L. Sha, C.-H. Liu, R.R. Alfano, Opt. Lett. **19**, 1922 (1994)
28. A.A. Ishchenko, N.A. Derevyanko, V.A. Svidro, Dyes Pigments **19**, 169 (1992)
29. V.A. Svetlichny, O.K. Bazyl, E.R. Kashapova, N.A. Derevyanko, A.A. Ishchenko, Q. Electron. **39**, 739 (2009)
30. A. Kobayashi, *Absolute Measurements of Photoluminescence Quantum Yields of Organic Compounds Using an Integrating Sphere* (Gunma University, Japan, 2010)
31. S. Schlücker (ed.), *Surface Enhanced Raman Spectroscopy: Analytical, Biophysical and Life Science Applications* (Wiley-VCH Verlag GmbH & Co. KGaA, Germany, 2011)
32. SPCImage. SPCImage3.9.4. *Data Analysis for Fluorescence Lifetime Imaging Microscopy* (Becker & Hickel, GmbH, Germany, 2012)
33. S.M. Kopylov, B.G. Lysoy, S.L. Seregin, O.B. Cherednichenko, Tunable dye lasers and their application (Radio and communication, Moscow, 1991) [in Russian]
34. O. Svelto, in *Principles of Lasers*, 4th edn., trans. and ed. by D.C. Hanna (Plenum, New York, 1998)
35. V.A. Rabinovich, Ya. Khavin, *Concise Handbook of Chemistry* (Khimiya, Leningrad, 1978). [in Russian]

**Publisher's Note** Springer Nature remains neutral with regard to jurisdictional claims in published maps and institutional affiliations.